Regional Applicability of Forest Height and Aboveground Biomass Models for the Geoscience Laser Altimeter System

Dirk Pflugmacher, Warren Cohen, Robert Kennedy, and Michael Lefsky

Abstract: Accurate estimates of forest aboveground biomass are needed to reduce uncertainties in global and regional terrestrial carbon fluxes. In this study we investigated the utility of the Geoscience Laser Altimeter System (GLAS) onboard the Ice, Cloud and land Elevation Satellite for large-scale biomass inventories. GLAS is the first spaceborne lidar sensor that will provide global estimates of forest height. We compared accuracy and regional variability of GLAS height estimates with data from the US Forest Service Inventory and Analysis (FIA) program and found that current GLAS algorithms provided generally accurate estimates of height. GLAS heights were on average 2–3 m lower than FIA estimates. To translate GLAS-estimated heights into forest biomass will require general allometric equations. Analysis of the regional variability of forest height-biomass relationships using FIA field data indicates that general nonspecies specific equations are applicable without a significant loss of prediction accuracy. We developed biomass models from FIA data and applied them to the GLAS-estimated heights. Regional estimates of forest biomass from GLAS differed between 39.7 and 58.2 Mg ha^{-1} compared with FIA. FOR. SCI. 54(6):647–657.

Keywords: lidar, Geoscience Laser Altimeter System, forest height, forest biomass, remote sensing

ACCURATE ESTIMATES of forest biomass, its spatial distribution, and rate of change are required to quantify global and regional terrestrial carbon fluxes and to formulate mitigation strategies for current and future greenhouse gas emissions. The global land-atmosphere C flux is currently most reliably estimated indirectly by deducting the residual between fossil fuel and cement emissions and the total uptake by the ocean and atmosphere (Denman et al. 2007). Direct observations of the carbon flux via flux measurements by the eddy covariance technique (Law et al. 2001) or biomass inventories (Goodale et al. 2002) are too sparse, given the heterogeneity of terrestrial ecosystems, to provide inferences with sufficient accuracy (Denman et al. 2007). National inventories provide the most extensive field observations and thus have been a key information source in many carbon studies (Goodale et al. 2002). However, their utility for global-scale studies is limited, because of methodological differences and the lack of observations in remote regions. There remain large areas in the tropics and the boreal zone for which inventory data are out of date or not available (Houghton 2005). In addition, most inventories are designed to provide inferences on the basis of administrative units or large regions. This is an important limitation, as information on carbon flux is needed on a spatial scale small enough to be linked to individual landscape units as they undergo natural disturbances, succession, or land-use changes (Houghton 2005). Consequently, the potential value of space-based observations is high.

Whereas spatially explicit and consistent earth observations are a primary strength of satellite remote sensing, remotely sensed estimation of forest biomass remains a challenging task (Lu 2006). Aboveground biomass is a three-dimensional variable. Hence, the capability of satellite sensors to provide accurate estimates depends on their ability to discriminate vertical forest structure. Many studies have demonstrated that canopy reflectance measured by passive optical sensors (Dong et al. 2003, Labrecque et al. 2006) and radar backscatter (Ranson et al. 1997) are correlated with aboveground biomass. However, both are two-dimensional measures and become asymptotic with canopy closure, limiting their ability to predict biomass in high biomass forests (Imhoff et al. 1998, Turner et al. 1999). Lidar and inferometric synthetic aperture radar (InSAR) are both promising technologies in that they provide a measure of the vertical structure. Nevertheless, InSAR has not yet achieved accuracies comparable to those with lidar (Treuhaft et al. 2004).

The success of airborne lidar systems in forest environments and the need for global observations has ultimately led to efforts first in the United States (Vegetation Canopy Lidar [VCL] mission) (Blair et al. 1999) and later in Germany (Carbon-3D mission) (Hese et al. 2005) to implement a space-based lidar mission for vegetation studies. Airborne simulations with the Laser Vegetation Imaging Sensor (LVIS), designed for the VCL space mission, achieved promising accuracies for estimating aboveground biomass at test sites in Costa Rica (root mean squared error [RMSE]

Dirk Pflugmacher, Oregon State University, Department of Forest Science, 321 Richardson Hall, Corvallis, OR 97331—Phone: (541) 750-7287; Fax: (541) 737-1393; dirk.pflugmacher@oregonstate.edu. Warren Cohen, US Forest Service, Pacific Northwest Research Station, Forestry Sciences Laboratory, 3200 SW Jefferson Way, Corvallis, OR 97331—warren.cohen@oregonstate.edu. Robert Kennedy, US Forest Service, Pacific Northwest Research Station, Forestry Sciences Laboratory, 3200 SW Jefferson Way, Corvallis, OR 97331—robert.kennedy@fs.fed.us. Michael Lefsky, Center for Ecological Analysis of Lidar, Department of Natural Resources, Colorado State University, 131 Forestry Building, Fort Collins, CO 80523-1472—lefsky@cnr.colostate.edu.

Acknowledgments: This research was funded by NASA's Terrestrial Ecology Program. We thank David Turner and three reviewers for their comments on an earlier draft of the manuscript.

Manuscript received October 29, 2007, accepted August 26, 2008

Copyright © 2008 by the Society of American Foresters

= 60.02–63.17 Mg ha^{-1}) Drake et al. 2002) and the United States (RMSE = 54.8–73.5 Mg ha^{-1}) (Hyde et al. 2005). Unfortunately, the two proposed missions did not receive funding from their space agencies.

In January 2003, the Ice, Cloud and land Elevation Satellite (ICESat) was launched as part of NASA's Earth Observing System of satellites to make global laser observations over the polar ice sheet, the land, the ocean, and the atmospheres (Zwally et al. 2002). ICESat carries a single sensor: the Geoscience Laser Altimeter System (GLAS). GLAS consists of three lasers operating in the near-infrared wavelength (1,064 nm) for measuring the elevation of surfaces and dense clouds and in the green wavelength (532 nm) for measuring the vertical distribution of clouds and aerosols.

An objective of the ICESat mission is to provide global measurements of canopy heights (Zwally et al. 2002). However, the size of the laser footprint is not optimal for vegetation studies (64-m diameter compared with 25-m diameter proposed for the VCL and Carbon-3D mission) because ICESat's primary mission is to monitor changes in elevation of the Greenland and Antarctic ice sheets. Nevertheless, a pilot study from Lefsky et al. (2005) demonstrated that GLAS is able to predict forest height (RMSE = 4.85–12.1 m) and biomass (RMSE = 58.3 Mg ha^{-1}) even in steep terrain. Recently, Rosette et al. (2008) estimated canopy heights with GLAS in a mixed temperate forest in the UK with an RMSE of 2.99 m.

In previous studies algorithms to transform GLAS waveform data into estimates of forest height were developed successfully, the applicability of such algorithms for regional inventories has not yet been explored. To produce a global canopy height data set, Lefsky et al. (2007) established a set of algorithm training sites currently located in North and South America. These sites were selected to represent a range of biomes and topographic conditions. Nevertheless, they cover only small areas with a limited number of waveforms. To determine the utility of GLAS for regional inventories, it is necessary to assess the accuracy of the canopy height algorithms outside the training sites and over a larger geographic extent.

GLAS estimates of forest canopy height will enable estimation of other forest attributes such as aboveground biomass. Several studies have shown that aboveground biomass is related to stand height (Drake et al. 2002, Lefsky et al. 1999, 2005). More extensive data sets, however, are needed to test the generality of such relationships in a regional and global context. The feasibility of estimating forest biomass with GLAS will ultimately depend on the availability and region of applicability of forest height-biomass equations. Because coarse-scale studies do not have the detailed information available as local studies, such equations need to be robust across a range of forest types and conditions. The objective of this study was to test the utility of GLAS data for regional forest biomass inventories by comparing GLAS estimates of forest height and biomass with existing forest inventory data and by exploring the region of applicability of GLAS height algorithms and forest height-biomass relationships.

Methods

Ideally, to evaluate the accuracy of height and biomass estimates, we would use reference data that have co-located GLAS waveforms and field-based height and biomass measurements. However, this approach is costly and therefore only feasible for a small sample of waveforms (i.e., for algorithm training sites). To validate the accuracy of GLAS estimates over a large geographic region therefore requires a different approach. Alternatively, national forest inventories provide extensive field measurements of forest height and biomass that can be used to validate GLAS estimates on a regional level.

In this study we used an approach that compared regional GLAS estimates of forest height and biomass with data from the US Forest Service Forest Inventory and Analysis (FIA) program at two large ecoregions in the Eastern and Western United States. We used the FIA data to develop plot-level height-biomass models, which we applied to the height estimates from GLAS, resulting in estimates of aboveground biomass for each GLAS sample. The region of applicability of height and biomass models within the study regions was evaluated by grouping FIA and GLAS samples into ecologically meaningful strata.

Study Regions

Our research was focused on the Cascade Mountains in the Pacific Northwest region and the Appalachian Mountains in the Southeast region of the United States (Figure 1). These two regions play an important role in the terrestrial carbon cycle and span a wide range of topographic and floristic conditions. The forests in the Cascade study region comprise mainly needleleaf trees, with Douglas-fir (*Pseudotsuga menziesii* [Mirb.] Franco) being the dominant species, followed by Sitka spruce (*Picea sitchensis* [Bong.] Carr.), mountain hemlock (*Tsuga mertensiana* [Bong.] Carr.), and lodgepole pine (*Pinus contorta* Dougl. ex. Loud.). In the Appalachian study region, broadleaf deciduous species dominate, e.g., oak (*Quercus* spp.) and hickory (*Carya* spp.).

The precise study region boundaries were determined on the basis of inventory data availability and the geographic extent of ecological sections and subsections (Table 1) as

Figure 1. Cascade (Western U.S.) and Appalachian study region (Eastern U.S.).

Table 1. Ecological sections and subsections of the study regions

Study Region and Ecological Section	Ecological Subsections
Cascades	
Western Cascades	West Cascade Slope Forest, Western Cascades Highland Forest, Cascade Crest Forest and Volcanic Peaks, Southern Oregon Cascades, Southern Oregon Cascade Highlands
Appalachians	
Southern Unglaciated Allegheny Plateau	Teays Plateau, Kinniconick and Licking Knobs
Northern Cumberland Plateau	Rugged Eastern Hills, Kinniconick and Licking Knobs, Southwestern Escarpment, Sequatchie Valley, Miami-Scioto Plain-Tipton Till Plain
Central Ridge and Valley	Rolling Limestone Hills
Southern Appalachian Piedmont	Schist Hills
Southern Cumberland Plateau	Shale Hills and Mountain, Sandstone Plateau, Table Plateau, Sandstone Mountain, Moulton Valley, Southern Cumberland Valleys
Southern Ridge and Valley	Chert Valley, Sandstone-Shale and Chert Ridge, Sandstone Ridge, Shaley Limestone Valley
Northern Ridge and Valley	Ridge and Valley, Great Valley of Virginia
Northern Cumberland Mountains	Western Coal Fields, Eastern Coal Fields, Black Mountains, Southern Cumberland Mountains, Pine and Cumberland Mountains
Blue Ridge Mountains	Northern Blue Ridge Mountains, Central Blue Ridge Mountains, Southern Blue Ridge Mountains, Metasedimentary Mountains

defined by the US Forest Service (McNab and Avers 1994). Because of the limited availability of recent statewide forest inventory data at the time of this analysis, the Cascade study region was confined to the state of Oregon. Similarly, the northern boundary of the Appalachian study region is bounded by the state borders of Kentucky and Virginia.

GLAS Data

GLAS includes a waveform digitizing lidar sensor. The instrument emits a laser pulse with an approximate footprint diameter of 64 m (Abshire et al. 2005). Within each footprint, laser energy is reflected back by all intercepting surfaces, resulting in a waveform that represents a vertical height profile of laser-illuminated surfaces.

In flat terrain and homogeneous forests, stand height is closely related to waveform extent, which is defined as the vertical distance between the first and last elevations at which the waveform energy exceeds a threshold level (Harding and Carabajal 2005). However, because of the relatively large GLAS footprint, the separation of the ground return from the vegetation surfaces is complicated in steep terrain and heterogeneous forest cover (Lefsky et al. 2005). The first algorithm that accounted for terrain effects incorporated a digital elevation model (Lefsky et al. 2005) and was a proof of concept that vegetation heights and biomass can be predicted from GLAS waveforms under complex terrain conditions.

The study presented here uses a new generation of height algorithms that do not require auxiliary topographic information but are based solely on the properties of the waveform (Lefsky et al. 2007). The height algorithms are calibrated to estimate the mean height of the dominant/codominant trees (dominant height) using field plots that coincide with GLAS samples. The coincident field plots that were used to train the height algorithms for the Cascade and Appalachian study regions are located in the Willamette National Forest and the Great Smoky Mountain National Park, respectively. For a more detailed description of the canopy height algorithms, see Lefsky et al. (2007).

Forest Inventory Data

Recent, annual field data from the US Forest Service FIA program were used as the reference data set, because they provide a nationally consistent and extensive data source suitable for landscape level studies. Field data are collected on permanent plots. Each plot consists of a set of four circular subplots, over which most tree measurements are taken. Trees with a dbh of 12.5 cm and larger are measured within a 7.3-m fixed radius, saplings (2.5–12.5 cm dbh) are measured on a 2-m microplot, and large trees (dbh $>$ 102 cm) are measured on an 18-m fixed-radius macroplot. For each plot, FIA field crews assign one or multiple condition classes based on a series of predetermined discrete variables such as land use, forest type, stand size, tree density, and ownership (Bechtold and Scott 2005). To avoid boundary plots (i.e., between forest/nonforest, forest types, or distinctly different successional stages), we selected only plots in which all four subplots were located completely on forestland and in the same condition class (Table 2).

Tree heights are measured in the field as the total length of a tree from the ground to the tip of the apical meristem. In some cases heights are visually estimated. Trees with estimated heights represented only a small proportion in this study (on average 3.6% per plot). For each plot, we calculated mean height of open grown, dominant, and codominant trees (dominant height), as this height metric was used to calibrate GLAS waveforms at the training sites. Identification of dominant and codominant trees is based on the

Table 2. Source and number of selected FIA plots

State	Report Year	Cycle	Subcycle	No. Plots
Alabama	2004	8	5/5	456
Georgia	2004	8	7/7	320
Kentucky	2004	5	5/5	603
North Carolina	2005	8	3/5	236
Oregon	2005	5	5/10	362
South Carolina	2001	3	5/5	30
Tennessee	2004	7	5/5	653
Virginia	2001	7	5/5	756

FIA crown class classification, which describes the position of a tree within the upper canopy layer (US Forest Service 2006). In addition to dominant height, we computed maximum height, as the height of the tallest tree, and mean height of all trees with dbh $\geq$ 2.5 cm.

We estimated total aboveground (oven-dry weight) biomass of all live trees (dbh $\geq$ 2.5 cm) for each inventory plot from a set of 10 allometric equations developed for coarse-scale studies (Jenkins et al. 2003). The "Jenkins equations" distinguish between four hardwood and six softwood species groups and use a simple log-linear regression model with dbh as the predictor variable. FIA also reports total aboveground tree mass, but these estimates are based on regional volume tables or models, and methodological differences (e.g., model form, parameter attributes, and nonlinear regression method) between FIA districts have been found to introduce regional biases (Hansen 2002). Conversely, the Jenkins equations are consistent in the way trees of defined dimension and species are treated across the United States. Although the uncertainty associated with these generalized equations is likely to be higher, it was more important in this study to use a consistent, regionally unbiased method to allow for regional comparisons. On rare occasions, trees have been measured at rootcollar (instead of dbh); in these cases the FIA biomass estimate was used. To obtain plot-level estimates of live aboveground biomass (Mg ha^{-1}), we multiplied the tree biomass values with a trees-per-acre expansion factor reported by FIA and calculated the sum of the biomass of all live trees per plot.

Estimation of Regional Parameters

We derived regional estimates of mean forest height and biomass using simple and stratified estimation. Both methods require a probability sampling design, e.g., random or systematic sample selection. FIA and GLAS feature systematic sampling. FIA uses a systematic sample on a hexagonal grid with an approximate spacing of 5.3 km, which is expected to produce a random, equal probability sample (Scott et al. 2005). We calculated stratified estimates of means and SEs using the standard formulas from Cochran (1977), ignoring finite population correction factors. Stratum weights were computed from digital maps showing forest/nonforest, forest type groups, and ecological subsections.

As for FIA, GLAS features systematic sampling. In contrast to airborne lidar instruments, GLAS does not provide images of canopy height but takes samples along transects (orbit tracks) every 172 m (center-to-center footprint spacing). The orbit tracks form a nonorthogonal grid spaced 14.5 km at the equator and 7 km at 60° latitude (Zwally et al. 2002). GLAS waveforms tend to saturate under cloudy sky conditions. Hence, the actual sampling density of cloud-free waveforms can vary.

We applied the GLAS height algorithms from Lefsky et al. (2007) to 18,346 cloud-free waveforms in the Cascade region and to 24,050 waveforms in the Appalachian study region acquired between October 2003 and November 2006. However, GLAS samples are very dense along transects such that neighboring observations could be spatially autocorrelated. The occurrence of spatial autocorrelation would violate the assumption of independence among samples. As a result, the sample mean computed for GLAS-derived forest height and biomass would not be an unbiased estimator, and the variance would be underestimated. To avoid spatial autocorrelation we randomly selected waveforms with the requirement that they be at least 2 km apart. We determined the minimum spacing on the basis of the range of a semivariogram from GLAS height estimates for each study region. We repeated sampling of the GLAS data 1,000 times for simple and stratified random estimation and calculated the mean of each sample using the same formulas as those we used for FIA. Thus, repeated sampling allowed us to construct a sampling distribution of the mean parameter. Mean and SD of that sampling distribution were used as estimates of the population mean and its SE.

Regional Applicability of GLAS Height Algorithms

We evaluated the regional performance of GLAS height algorithms by comparing the frequency distributions of GLAS-estimated heights and FIA-estimated dominant heights for each study region. GLAS heights less then 2 m and over nonforest land (National Land Cover Data [NLCD], 2001) were omitted from the analysis. The NLCD is a Landsat-based land cover map for the conterminous United States that distinguishes these forest classes: deciduous, evergreen, and mixed forests as well as woody wetlands. We further compared mean FIA and GLAS estimates by forest type group and ecological subsection. The two variables are reported in the FIA database and are also available as geospatial data layers. We used the latter to determine the respective membership for the GLAS samples.

Forest type groups are aggregations of forest types into ecological groupings (Eyre 1980). The US Forest Service distinguishes 28 national forest type groups. Forest types are specified by FIA for each plot condition. Because we analyzed only plots with unique condition classes, each plot was associated with a single forest type group. The corresponding spatial layer is a thematic map produced with data from the Moderate Resolution Imaging Spectroradiometer acquired in 2001 at a spatial resolution of 250 m (US Forest Service 2007, Ruefenacht et al. 2008). We used this map to determine forest type groups for the GLAS samples.

Whereas the comparison by forest type groups explores the effect of tree species and species groups on the performance of the GLAS algorithm, the meaning of ecological subsections is more complex. Ecological subsections are geographic regions of similar surficial geology, lithology, geomorphic process, soil groups, subregional climate, and potential natural communities (US Forest Service 2006). A vector layer is available for download (US Forest Service, 2005).

Assuming that the FIA provided an unbiased estimate of the mean height for each stratum, we calculated the bias of the GLAS estimate as the difference between the GLAS and FIA mean. To obtain reliable stratified estimates, a minimum of five plots per stratum is recommended by the FIA

(McRoberts 2006). Therefore, forest type groups with fewer than five plots were omitted from this analysis (see Table 3 for sample sizes). No ecological subsections contained less than five plots.

For each ecological subsection, we determined mean slope and elevation from a 30-m digital elevation model to explore potential biases introduced by differences in terrain conditions. Also, given the size of the study regions, there may be biases that are indirectly related to the distance of the GLAS samples from the source of the height calibration data set. To test for this effect, the proximity of each ecological subsection to the training site for the height calibration data set was calculated (as the Euclidean distance between the geographic center of each subsection and the geographic center of the subsection containing the training data). Proximity was only calculated for the Appalachian study region. Because of the spatial arrangement and low number of ecological subsections in the Cascade region, a proximity measure was not meaningful.

Regional Applicability of Height-Biomass Models

The regional applicability of height-based allometric equations to predict forest biomass largely depends on the site-specific variability in the relationship between plot-level height and biomass. For each study region, we developed height-based biomass regression models using FIA plot data and then tested the region of model applicability (as for the height algorithms) using information on forest type groups and ecological subsections.

To develop a basic height-biomass model, we log-transformed the predictor and response variables and fitted a linear regression model. We then included the factors forest type group and ecological subsection using indicator variables and multiple linear regression models with and without interaction terms. Addition of these variables permitted the mean response (biomass) in the models to vary with different levels of the factors. We evaluated all models on the basis of several statistics: the model's coefficient of determination, and the RMSE and bias of the predicted versus observed values. Bias was calculated as the mean of the predicted values minus the mean of the observed values.

When factors are included in regression models, the sample is partitioned into groups according to the number of factor levels. As a result some of the groups may contain only a few observations. To assure an adequate sample size for each factor level, we excluded forest type groups and ecological subsections with fewer than 10 observations. As a result, 4 of 10 and 7 of 10 forest type groups remained for analysis in the Cascade and Appalachian study region, respectively (see Table 3 for sample sizes). In addition, one of the 33 ecological subsections located in the Appalachian region had less than 10 plots and was removed.

We developed and tested regression models based on dominant, maximum, and mean height, respectively. Because GLAS provides estimates of dominant height,

Table 3. Means and SEs of FIA (dominant height) and GLAS heights by forest type group in the Cascade and the Appalachian study region

		FIA height (m)			GLAS height			
Forest type group	Area	Mean	SE	No. plots	Mean	SE	No. shots	Bias
	(10^3 ha)	(m)						
Cascades								
Douglas-fir	2,021.08	32.11	1.07	181	26.62	0.27	725.3	−5.5
Ponderosa pine	17.53	22.60	3.90	7	13.60	1.54	3.5	−9.0
Western white pine	0.10	30.08		1				
Fir/spruce/mountain hemlock	657.86	23.48	0.78	122	21.80	0.41	238.9	−1.7
Lodgepole pine	62.93	17.07	1.12	16	11.62	0.88	23.5	−5.4
Hemlock/sitka spruce	25.01	30.02	2.76	26	24.66	1.43	26.3	−5.4
Other western softwoods	0.54	16.60		1				
California mixed conifer	1.69				7.34	0.86	1.0	
Elm/ash/cottonwood	0.04							
Aspen/birch	0.08							
Alder/maple	0.69	17.81	5.24	3	20.89	0.48	4.0	3.1
Western oak	0.76				22.36	0.50	1.0	
Tanoak/laurel	0.04	12.05	4.26	2				
Other western hardwoods	0.07	10.12	4.51	3				
Appalachians								
White/red/jack pine	95.93	21.59	0.83	74	18.21	0.56	30.4	−3.4
Spruce/fir	0.01	19.18	1.97	7				
Longleaf/slash pine	9.96	15.65	3.71	4	9.99	1.16	2.0	−5.7
Loblolly/shortleaf pine	758.29	14.13	0.40	229	14.20	0.22	272.5	0.1
Pinyon/juniper	2.23	12.03	1.00	9				
Oak/pine	427.99	17.86	0.34	277	16.22	0.22	211.9	−1.6
Oak/hickory	12,128.11	21.49	0.11	2,348	17.52	0.10	1,863.9	−4.0
Oak/gum/cypress group	34.64	21.02	1.85	13	14.61	0.73	19.0	−6.4
Elm/ash/cottonwood	21.24	21.02	1.06	13	15.75	0.87	9.0	−5.3
Maple/beech/birch	100.28	22.96	0.49	80	16.68	0.54	16.7	−6.3

GLAS statistics are based on 1000 random samples with a mean sample size = No. shots. Bias is the difference between the mean GLAS and mean FIA estimate.

empirical relationships between biomass and this height metric were of primary interest. However, we also developed models using maximum and mean height as predictor variables and compared their performance.

Regional Estimates of Forest Biomass

To estimate forest biomass for each GLAS sample, we calibrated plot-level height-biomass models using FIA data and applied the "best" regional model to the GLAS estimates of height. Then we calculated and compared mean estimates of forest biomass from GLAS and FIA data using simple and stratified estimation by forest type groups and ecological subsections. Forest area for the ecological subsections was determined from the NLCD 2001.

Because a minimum of five plots per stratum is considered necessary for reliable stratified estimates (McRoberts 2006), we combined strata with fewer than five plots with ecologically similar strata. For FIA estimates in the Cascade region, we combined the western white pine and the other western softwoods group with the ponderosa pine group and the alder/maple and tanoak/laurel group with the other western hardwoods group. In the Appalachian region, it was necessary to pool together the longleaf/slash pine group with the loblolly/shortleaf pine group. For stratified GLAS estimates we combined the California mixed conifer group and the ponderosa pine group with the lodgepole pine group, the western oak group with the alder/maple group, and the longleaf/slash pine group with the loblolly/shortleaf pine group.

Results

Regional Applicability of GLAS Height Algorithms

Repeated random sampling from the GLAS data resulted for each study region in 1,000 subsamples with average sample sizes of 863 and 1,948 shots for the Cascade and Appalachian region, respectively. The FIA sample consisted of 362 forest plots in the Cascade and 3,054 forest plots in the Appalachian study region. Comparison of the frequency distributions of GLAS heights, which show the mean frequency of 1,000 sample distributions, with frequency distributions from FIA suggested that the GLAS algorithms generally were accurate predictors of dominant height (Figure 2). In the Cascade region, the GLAS estimate of mean forest height was 25.3 m (±0.5 m 95% CI), which is 2.4 m lower than the FIA estimate of the mean (27.7 ± 1.4 m). The agreement is higher between the medians of the two distributions (difference of 0.8 m) and also very good between the maximum heights (FIA: 65.7 m, GLAS mean of all subsample maxima: 64.7 m, and GLAS maximum of all waveforms: 69.7 m). However, the frequency of FIA heights was higher in the height range between 30 and 55 m compared with GLAS.

In the Appalachian region the GLAS estimate of mean forest height was 3.3 m lower than the FIA estimate (GLAS: 17.3 m ± 0.2 m and FIA: 20.6 m ± 0.2 m). Both frequency distributions are symmetric and exhibit similar standard deviations (FIA: 5.8 m and GLAS: 6.5 m). The maximum observed height of the 1,000 GLAS subsamples was 51.6 m (or 58.5 m when all GLAS waveforms are considered). Compared with FIA (39.8 m), this is a difference of 11.8 m. However, the majority of height estimates were within a similar range: 98% of the height estimates were between 3.4 and 34.0 m (GLAS) and between 4.6 and 33.4 m (FIA), respectively.

Examination of GLAS height distributions sampled by forest type groups revealed no substantive bias associated with tree species composition (Table 3). In the Cascade region, differences between GLAS and FIA heights varied from −5.4 to −1.7 m for forest types with more than five plots. The bias of the Douglas-fir group, which was associated with the GLAS training plots, is nearly equivalent to the average bias across forest types (−4.5 m). The largest differences were observed in forest type groups with small sample sizes from FIA and GLAS (hemlock/Sitka spruce and lodgepole pine groups). The results are similar in the Appalachian region with biases varying between −6.4 and 0.1 m. In comparison, biases of the forest type groups associated with the training plots were −1.6 and −4.0 m (oak/pine group and oak/hickory forest groups, respectively). Again, the largest differences occurred in groups with small sample sizes (oak/gum/cypress and elm/ash/cottonwood groups).

An analysis of the mean differences between FIA- and GLAS-estimated heights by ecological subsection revealed no association between biases and median topographic

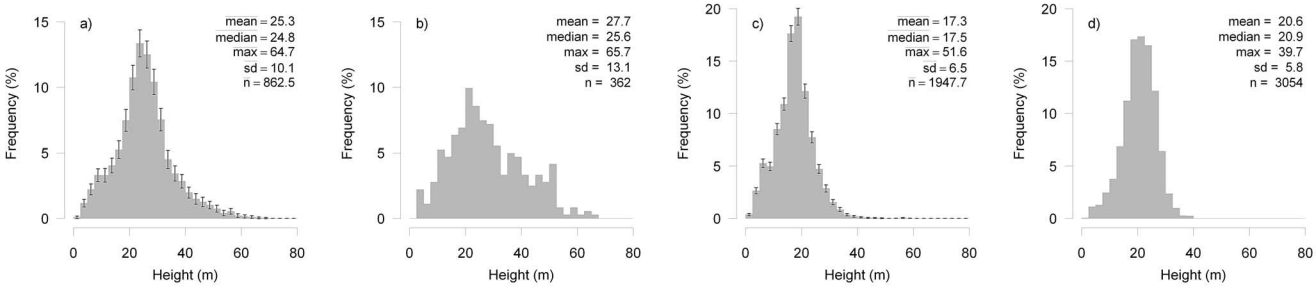

Figure 2. Frequency distributions for forest height in the Cascade (a, b) and Appalachian study region (c, d). Panels a and c show the mean frequency and the standard error for 1,000 repeated, random GLAS samples. Estimates of the mean, median, maximum (max), and SD (sd) depict the mean of these estimates across the 1,000 samples, which have a mean sample size of size = $\bar{n}$. Panels b and c show the frequency distributions of FIA samples based on dominant height.

slope, median elevation, or proximity to training data set (Figure 3a–c). In the ecological subsection containing the training plots of the Appalachian region, for example, GLAS-estimated heights were on average −3.4 m lower than FIA heights. In comparison, we determined a difference of −4.0 m for the most distant subsection. Again, the largest biases occurred in subsections with limited FIA plot representation (as in the forest type groups). These subsections also exhibited the largest standard errors in the GLAS and FIA estimates (Figure 3d–f).

Regional Applicability of Height-Biomass Models

Empirical analysis of the height-biomass relationships revealed that the general region-specific allometic equations predicted biomass with accuracies comparable to those with forest type-specific and ecological subsection-specific equations. All regression models performed similarly across the study regions, in that there were only slight differences in model fit and prediction accuracy by factor and factor level (Table 4). The coefficient of determination of models using dominant height, for example, varied between 0.74 and 0.77 in the Cascade study region and between 0.60 and 0.64 in the Appalachian study region. Model fit and prediction accuracy improved in both regions when variations in forest type and ecological subsection were taken into account; however, these improvements were minimal. For example, RMSEs decreased between 6.6 and 12.2 Mg ha^{-1} in the Cascade region and between 2.9 and 3.8 Mg ha^{-1} in the Appalachian region, depending on the height metric used. These amounts correspond to less than 4% of the mean observed aboveground biomass in each study area (334 and 148 Mg ha^{-1} in the Cascade and Appalachian regions, respectively).

The performance of models using dominant height was similar to that of models based on mean or maximum height. However, differences were greater in the Cascade region with higher biomass forests than in the Appalachian region. In the Cascade region, prediction accuracies of maximum height models were between 0.8 and 6.0 Mg ha^{-1} better than the accuracies of dominant height models. Conversely, maximum height produced biases 2–3 times as high as the biases observed with dominant height. Finally, models using mean height were least accurate with RMSE values between 32.5 and 41.4 Mg ha^{-1} greater than the RMSE values for dominant height models. In the Appalachian region, differences between all height metrics were minimal and did not exceed 1.7 Mg ha^{-1}.

Because accounting for variations in ecological subsections and forest type groups did not improve the prediction accuracy of the models significantly, we proceeded with the simplest model that used dominant height as a single predictor variable. We recalculated the model parameters including all plots from all forest type groups and ecological subsections. The resulting models explained 74 and 60% of the variation in the FIA biomass data in the Cascade and Appalachian region, respectively. The equations are as follows (SEs are shown in square brackets):

$$\mathrm{AGBM}_C = \exp(0.155[0.168] + 1.665[0.052] \cdot \ln(\text{height})), \quad (1)$$

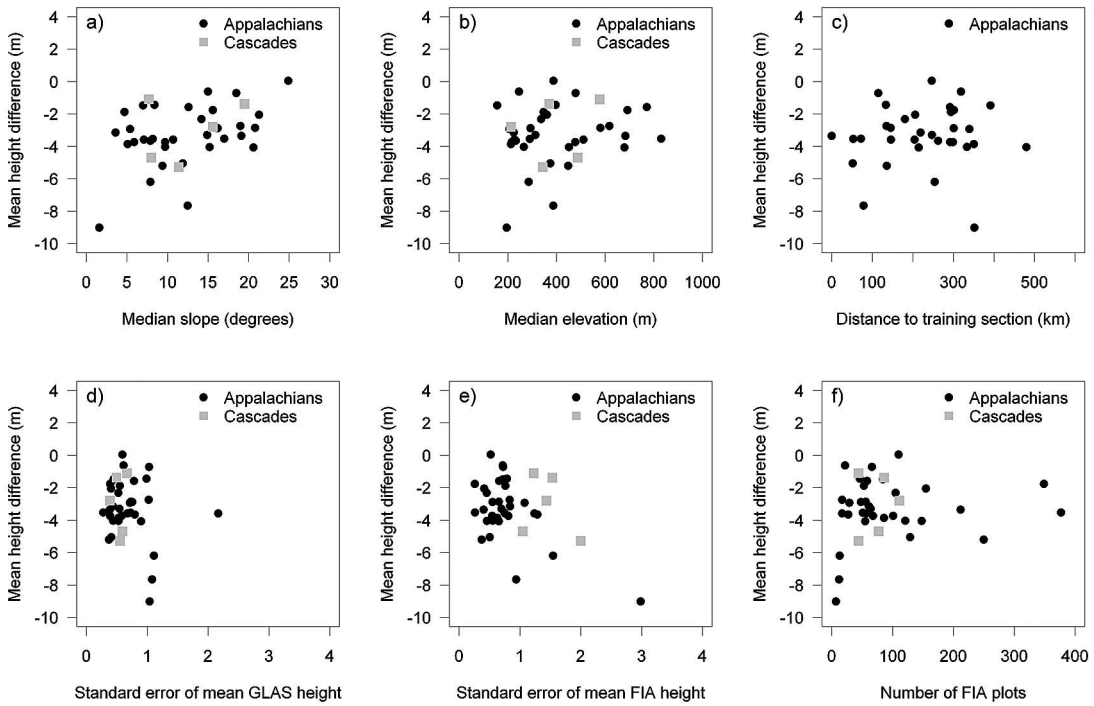

Figure 3. Scatterplots showing the bias (difference) between mean GLAS and mean FIA height at the ecosubsection level versus (a) median slope and (b) elevation of forested area, (c) distance to the geographic center of the ecological subsection with the training data, (d) standard error of mean GLAS height, (e) standard error of FIA dominant height, and (f) number of FIA plots.

Table 4. Comparison of biomass models that account for forest type group or ecological subsection or both with and without interaction

Model terms	Cascades			Appalachians		
	RMSE	BIAS	R^2	RMSE	BIAS	R^2
log(d-ht)	173.13	−3.43	0.74	60.58	−7.53	0.60
log(d-ht)*ecosubcd	168.71	−6.06	0.76	57.31	−7.09	0.64
log(d-ht)*fortypgrp	165.52	−6.04	0.76	60.84	−7.54	0.60
log(d-ht)*fortypgrp + log(d-ht)*ecosubcd	164.60	−7.16	0.77	58.02	−6.79	0.64
log(d-ht)+ecosubcd	166.37	−5.52	0.75	58.61	−6.53	0.62
log(d-ht)+fortypgrp	164.96	−6.08	0.76	61.13	−7.38	0.60
log(d-ht)+fortypgrp + ecosubcd	162.69	−6.34	0.76	59.49	−6.30	0.63
log(max-ht)	167.13	−15.57	0.73	61.49	−8.94	0.59
log(max-ht)*ecosubcd	164.71	−16.58	0.74	58.69	−8.47	0.63
log(max-ht)*fortypgrp	164.75	−18.01	0.74	61.95	−8.72	0.59
log(max-ht)*fortypgrp + log(max-ht)*ecosubcd	162.72	−17.52	0.74	59.69	−7.86	0.64
log(max-ht)+ecosubcd	161.50	−17.47	0.74	60.02	−7.84	0.61
log(max-ht)+fortypgrp	164.15	−17.49	0.74	62.11	−8.77	0.59
log(max-ht)+fortypgrp + ecosubcd	160.52	−17.76	0.74	61.10	−7.53	0.62
log(mean-ht)	205.59	−5.71	0.67	61.54	−8.02	0.57
log(mean-ht)*ecosubcd	210.09	−5.91	0.71	58.61	−7.65	0.61
log(mean-ht)*fortypgrp	200.67	−6.04	0.71	61.05	−8.27	0.57
log(mean-ht)*fortypgrp + log(mean-ht)*ecosubcd	200.41	−7.45	0.73	58.94	−7.60	0.61
log(mean-ht)+ecosubcd	204.16	−5.55	0.70	59.57	−7.12	0.59
log(mean-ht)+fortypgrp	201.07	−6.17	0.71	61.53	−7.96	0.57
log(mean-ht)+fortypgrp + ecosubcd	197.87	−6.21	0.71	59.98	−7.02	0.59

Plot heights are defined as height of the tallest tree (max-ht), mean height (mean-ht), and dominant height (d-ht). Model evaluation is based on the RMSE and BIAS of the predicted (fitted) versus observed biomass values, and the R^2 of the regression model. fortypgrp, forest type group; ecosubcd, ecological subsection; *, with interaction; +, without interaction.

$$\mathrm{AGBM}_A = \exp(-0.484[0.079] + 1.777[0.026] \cdot \ln(\text{height})), \quad (2)$$

$\mathrm{AGBM_C}$ and $\mathrm{AGBM_A}$ are total aboveground (oven-dry weight) biomasses (Mg ha^{-1}) for the Cascade and Appalachian region, respectively, height is the dominant height (m), exp is an exponential function, and ln is the logarithm base e (2.71842).

The Cascade model had a bias of −2.66 Mg ha^{-1} and yielded an RMSE of 174.7 Mg ha^{-1}, which corresponds to 12.0% of the maximum and 52.3% of the mean observed biomass value. In comparison, the bias of the Appalachian model was −7.52 Mg ha^{-1} with an RMSE of 60.6 Mg ha^{-1}, which corresponds to 11.2% of the maximum and 40.9% of the mean biomass of this region (Figure 4).

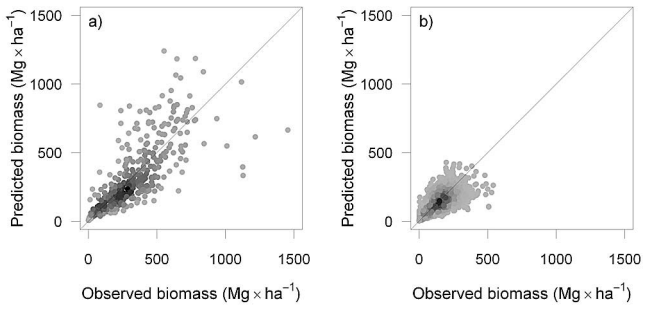

Figure 4. Observed versus predicted aboveground biomass (Mg ha^{-1}) for the Cascade (left, RMSE = 174.7 Mg ha^{-1}, n = 362) and Appalachian study region (right, RMSE = 60.6 Mg ha^{-1}, n = 3,054)

Regional Biomass Estimates

To obtain regional estimates of mean aboveground biomass, we applied the regional biomass models (equations 1 and 2) based on FIA data to the GLAS heights. Table 5 shows the regional estimates of biomass from GLAS and FIA data based on simple and stratified estimation. Simple estimates of biomass from GLAS were 40.9 and 58.2 Mg ha^{-1} lower than estimated by FIA in the Appalachian and Cascade region, respectively (27.6 and 17.4% of the FIA mean, respectively). Stratification by forest type or ecological subsection did not decrease standard errors of the estimates or the discrepancy between FIA and GLAS significantly. The results are in agreement with our previous

Table 5. Means and SEs of the regional biomass estimates from GLAS and FIA based on simple and stratified estimation

Region and Estimation method	Biomass FIA		Biomass GLAS	
	Mean	SE	Mean	SE
	. . . . . .Mg ha^{-1}.			
Appalachians				
Simple, no strata	148.06	1.33	107.20	1.06
Stratified by ecosubsection	148.92	1.29	109.19	1.14
Stratified by forest type group	150.98	1.35	106.80	1.02
Cascades				
Simple, no strata	334.03	11.75	275.87	4.61
Stratified by ecosubsection	336.50	12.06	270.91	4.07
Stratified by forest type group	352.85	13.85	272.90	4.11

findings (section Regional Applicability of Height-Biomass Models), that differences between FIA- and GLAS-estimated heights are not explained by this type of stratification.

Discussion

In this study, we validated the regional applicability of height algorithms for the GLAS sensor. The height algorithms used here correspond to two training sites located in the Cascade and Appalachian regions in the United States. According to Lefsky et al. (2007), GLAS algorithms explained 90% (Cascades) and 40% (Appalachians) of the variance in the training data with RMSEs of 5.91 m (Cascades) and 4.86 m (Appalachians), respectively. The results of our study show good agreement between GLAS and FIA dominant heights, despite the relatively few plots available for direct calibration of GLAS height algorithms. GLAS heights are on average 2–3 m lower than FIA heights. We were not able to detect any patterns of disagreement associated with forest type, mean slope, elevation, or proximity of training data. Further research will need to focus more specifically on the GLAS waveforms and their response to varying forest structure and topographic conditions. This will require additional training sites (potentially with high-resolution lidar data) and simulation exercises (Yong, P., and M. Lefsky, in preparation).

To explore the regional accuracy of GLAS-estimated forest heights, we built on an approach that compared regional distributions of forest heights with data from the US Forest Service FIA program. We choose this approach because it had a large geographic scope, and it provided inferences on an application-oriented level. However, the results of this study were not only influenced by the accuracy of the height algorithms but also by potential other factors that could be inherent to the GLAS data (e.g., a temporal or spatial inconsistency) or the sampling scheme (e.g., sampling bias). An additional weakness of this region-level analysis was its limited flexibility in linking the uncertainties of the height estimates to potentially important environmental factors (e.g., stand structure and terrain conditions). To obtain site-specific inferences will require reference measurements coincident with GLAS samples. However, because neither field nor high-resolution lidar data are currently available for extensive areas, such a study would be confined to small geographic regions.

We explored the regional applicability of height-biomass allometic equations and found that regional models based on height as a single predictor variable performed as well as models that accounted for variations in forest types and ecological subsections. This finding suggests that generalized, nonsite- and nonspecies-specific allometric equations can be useful for coarse-scale estimation of forest biomass. The hypothesis of a universal equation that relates canopy height and biomass has been formulated by Lefsky et al. (2002). They found that their lidar height-biomass relationships were robust across the forest types investigated and even major biomes. However, their findings were based on only a limited number of samples and should be considered preliminary. This study represents a more rigorous test with a more extensive data set. Similarly, Mette et al. (2003) compared height-based equations for two hardwood and two coniferous tree species using German forest yield tables and found that the overall variability in the equations between species and stand ages was negligible ($<15\%$). In this study we developed separate equations for study regions dominated by coniferous and broadleaf forests. Thus, we did not attempt to draw inferences across these two types of forests. Nevertheless, the results are promising as it is unlikely that accurate and global fine-scale maps for tree species composition will be available in the near future. We do anticipate that stand density, canopy cover, and perhaps a classification by leaf type might reduce the residual variance observed in our biomass models. However, more research is required to quantify these effects. Conventional remote sensing has been successful in retrieving such two-dimensional variables. Future research should focus on possible synergies of GLAS with other sensor technologies.

Accuracies for estimating canopy heights and forest biomass with GLAS were lower than those typically achieved with airborne, small footprint lidar sensors (e.g., RMSE = 8.1 Mg ha^{-1}) (Lim and Treitz, 2004), which makes GLAS less suitable for local studies. Regional biomass estimates obtained from GLAS were between 17.4 and 27.6% lower than FIA estimates. However, GLAS estimates would be a valuable and unique data source for inventorying canopy height and biomass stocks on a global scale and in areas that have previously been difficult to monitor. These areas include remote forests of Canada and Russia and large areas in the tropics (Houghton 2005). It is difficult to define what level of accuracy is required to reduce the current uncertainty in the global carbon flux (Houghton 2005). According to Houghton (2005), estimating aboveground biomass to within 10–25% might reduce the current uncertainty in the carbon flux to a similar range, which is currently $>100\%$.

There are sources of error related to the measurements and allometric equations at the tree-level that may propagate to the plot and landscape level, but they are not specific to GLAS and thus were beyond the scope of this study. Because the study regions in this research were selected to include complex terrain and high biomass forests, the results obtained here might represent the lower limit of accuracy that can be expected with GLAS.

This study focused on regional estimates, obtained by averaging individual GLAS estimates over a larger geographic region. Given the relatively high prediction error in the plot-level relationships between canopy height and forest biomass, which was approximately 50% of the mean observed biomass value in both regions (RMSE = 60.6 and 174.7 Mg ha^{-1}), some aggregation of individual GLAS observations is necessary to increase the confidence in the biomass estimates from GLAS. At the regional scale, the uncertainty in the biomass models had only a little effect on the estimate of the mean (biases: -2.66 and -7.52 Mg ha^{-1}). It remains to be tested how large an area (or grain size) is necessary to obtain a robust biomass estimate while still being fine enough to capture processes of land use change and natural disturbances.

There are great uncertainties in the current and future ability of forest ecosystems to offset anthropogenic carbon

emissions. New approaches are required to improve our knowledge on the distribution of plant biomass across the globe. With the GLAS onboard NASA's ICESat satellite, now global lidar observations have become available that could potentially be used in global and coarse-scale vegetation studies. Furthermore, GLAS provides a means to study the data and mission requirements for future spaceborne lidar instruments. The Committee on Earth Science and Applications from Space: A Community Assessment and Strategy for the Future and the National Research Council (2007) have included in their recommendation for the next decade of space missions two operations that could support lidar observations of forests. Existing inventory programs such as the FIA will be an important tool to provide the field observations necessary for validation.

Literature Cited

ABSHIRE, J.B., X.L. SUN, H. RIRIS, J.M. SIROTA, J.F. MCGARRY, S. PALM, D.H. YI, AND P. LIIVA. 2005. Geoscience Laser Altimeter System (GLAS) on the ICESat mission: On-orbit measurement performance. *Geophys. Res. Lett.* 32(21): doi:10.1029/2005GL024028.

BECHTOLD, W.A., AND C.T. SCOTT. 2005. The Forest Inventory and Analysis plot design. P. 27–42 in *The Enhanced Forest Inventory and Analysis program—National sampling design and estimation procedures*, Bechtold, W.A., and P.L. Patterson (eds.). US For. Serv. Gen. Tech. Rep. SRS-80. 98 p.

BLAIR, J.B., D.L. RABINE, AND M.A. HOFTON. 1999. The Laser Vegetation Imaging Sensor: a medium-altitude, digitization-only, airborne laser altimeter for mapping vegetation and topography. *ISPRS J. Photogramm.* 54(2–3):115–122.

COCHRAN, W.G. 1977. *Sampling techniques*, 3rd ed. John Wiley & Sons, New York, NY. 428 p.

COMMITTEE ON EARTH SCIENCE AND APPLICATIONS FROM SPACE: A COMMUNITY ASSESSMENT AND STRATEGY FOR THE FUTURE, AND NATIONAL RESEARCH COUNCIL. 2007. *Earth science and applications from space: National imperatives for the next decade and beyond.* National Academies Press, Washington, DC. 456 p.

DENMAN, K.L., G. BRASSEUR, A. CHIDTHAISONG, P. CIAIS, P.M. COX, R.E. DICKINSON, D. HAUGLUSTAINE, C. HEINZE, E. HOLLAND, D. JACOB, U. LOHMANN, S. RAMACHANDRAN, P.L. DA SILVA DIAS, S.C. WOFSY, AND X. ZHANG. 2007. Couplings between changes in the climate system and biogeochemistry. P. 499–587 in *Climate change 2007: The physical science basis. Contribution of working group I to the fourth assessment report of the Intergovernmental Panel on Climate Change*, Solomon, S., D. Qin, M. Manning, Z. Chen, M. Marquis, K.B. Averyt, M. Tignor, and H.L. Miller (eds.). Cambridge University Press, Cambridge, UK.

DONG, J.R., R.K. KAUFMANN, R.B. MYNENI, C.J. TUCKER, P.E. KAUPPI, J. LISKI, W. BUERMANN, V. ALEXEYEV, AND M.K. HUGHES. 2003. Remote sensing estimates of boreal and temperate forest woody biomass: carbon pools, sources, and sinks. *Remote Sens. Environ.* 84(3):393–410.

DRAKE, J.B., R.O. DUBAYAH, R.G. KNOX, D.B. CLARK, AND J.B. BLAIR. 2002. Sensitivity of large-footprint lidar to canopy structure and biomass in a neotropical rainforest. *Remote Sens. Environ.* 81(2–3):378–392.

EYRE, F.H. 1980. *Forest cover types of the United States and Canada.* Society of American Foresters, Bethesda, MD. 148 p.

GOODALE, C.L., M.J. APPS, R.A. BIRDSEY, C.B. FIELD, L.S. HEATH, R.A. HOUGHTON, J.C. JENKINS, G.H. KOHLMAIER, W. KURZ, S.R. LIU, G.J. NABUURS, S. NILSSON, AND A.Z. SHVIDENKO. 2002. Forest carbon sinks in the northern hemisphere. *Ecol. Appl.* 12(3):891–899.

HANSEN, M. 2002. Volume and biomass estimation in FIA: national consistency vs. regional accuracy. P. 109–120 in *Proc. of the Third annual forest inventory and analysis symposium*, McRoberts, R.E., G.A. Reams, P.C. Van Deusen, and J.W. Moser (eds.). US For. Serv. Gen. Tech. Rep. NC-230. 216 p.

HARDING, D.J., AND C.C. CARABAJAL. 2005. ICESat waveform measurements of within-footprint topographic relief and vegetation vertical structure. *Geophys. Res. Lett.* 32(21): doi:10.1029/2005GL023471.

HESE, S.M., W. LUCHT, C. SCHMULLIUS, M. BARNSLEY, R. DUBAYAH, D. KNORR, K. NEUMANN, T. RIEDEL, AND K. SCHRÖTER. 2005. Global biomass mapping for an improved understanding of the CO_2 balance—The Earth observation mission Carbon-3D. *Remote Sens. Environ.* 94:94–104.

HOUGHTON, R.A. 2005. Aboveground forest biomass and the global carbon balance. *Glob. Change Biol.* 11(6):945–958.

HYDE, P., R. DUBAYAH, B. PETERSON, J.B. BLAIR, M. HOFTON, C. HUNSAKER, R. KNOX, AND W. WALKER. 2005. Mapping forest structure for wildlife habitat analysis using waveform lidar: Validation of montane ecosystems. *Remote Sens. Environ.* 96(3–4):427–437.

IMHOFF, M.L., S. CARSON, AND P. JOHNSON. 1998. A low-frequency radar experiment for measuring vegetation biomass. *IEEE Trans. Geosci. Remote Sens.* 36(6):1988–1991.

JENKINS, J.C., D.C. CHOJNACKY, L.S. HEATH, AND R.A. BIRDSEY. 2003. National-scale biomass estimators for United States tree species. *For. Sci.* 49(1):12–35.

LABRECQUE, S., R.A. FOURNIER, J.E. LUTHER, AND D. PIERCEY. 2006. A comparison of four methods to map biomass from Landsat-TM and inventory data in Western Newfoundland. *For. Ecol. Manag.* 226(1–3):129–144.

LAW, B.E., P.E. THORNTON, J. IRVINE, P.M. ANTHONI, AND S. VAN. TUYL. 2001. Carbon storage and fluxes in ponderosa pine forests at different developmental stages. *Global Change Biol.* 7(7):755–777.

LEFSKY, M.A., W.B. COHEN, D.J. HARDING, G.G. PARKER, S.A. ACKER, AND S.T. GOWER. 2002. Lidar remote sensing of above-ground biomass in three biomes. *Global Ecol. Biogeogr.* 11(5):393–399.

LEFSKY, M.A., D. HARDING, W.B. COHEN, G. PARKER, AND H.H. SHUGART. 1999. Surface lidar remote sensing of basal area and biomass in deciduous forests of Eastern Maryland, USA. *Remote Sens. Environ.* 67(1):83–98.

LEFSKY, M.A., D.J. HARDING, M. KELLER, W.B. COHEN, C.C. CARABAJAL, F.D. ESPIRITO-SANTO, M.O. HUNTER, R. DE OLIVEIRA, AND P.B. DE CAMARGO. 2005. Estimates of forest canopy height and aboveground biomass using ICESat. *Geophys. Res. Lett.* 32(22): doi:10.1029/2005GL023971.

LEFSKY, M.A., M. KELLER, Y. PANG., P.B. DE CAMARGO, M.O. HUNTER. 2007. Revised method for forest canopy height estimation from Geoscience Laser Altimeter System waveforms. *J. Appl. Rem. Sens.* 1(1):013537-18.

LIM, K., AND P. TREITZ. 2004. Estimation of aboveground forest biomass from airborne discrete return laser scanner data using canopy-based quantile estimators. *Scand. J. For. Res.* 19: 558–570.

LU, D.S. 2006. The potential and challenge of remote sensing-based biomass estimation. *Int. J. Remote Sens.* 27(7): 1297–1328.

MCNAB, W.H., AND P.E. AVERS. 1994. *Ecological subregions of*

the United States: Section descriptions. US For. Serv. WO-WSA-5. Available online at www.fs.fed.us/land/pubs/ecoregions/; last accessed Jan. 26, 2007.

MCROBERTS, R.E. 2006. A model-based approach to inventory stratification. P. 126 in *Proc. of the Sixth annual forest inventory and analysis symposium*, McRoberts, R.E., G.A. Reams, P.C. Van Duesen, and W.H. McWilliams (eds.). US For. Serv. Gen. Tech. Rep. WO-70. 132 p.

METTE, T., K.P. PAPATHANASSIOU, I. HAJNSEK, AND R. ZIMMERMANN. 2003. Forest biomass estimation using polarimetric SAR interferometry. in *Proc. of the Workshop on POLinSAR—Applications of SAR polarimetry and polarimetric interferometry (ESA SP-529*). Jan. 14–16, 2003, Frascati, Italy. Published on CD-ROM, p.23.1.

RANSON, K.J., G. SUN, R.H. LANG, N.S. CHAUHAN, R.J. CACCIOLA, AND O. KILIC. 1997. Mapping of boreal forest biomass from spaceborne synthetic aperture radar. *J. Geophys. Res.* 102(D24):29599–29610.

ROSETTE, J.A.B., P.R.J. NORTH, AND J.C. SUAREZ. 2008. Vegetation height estimates for a mixed temperate forest using satellite laser altimetry. *Int. J. Remote Sens.* 29(5):1475–1493.

RUEFENACHT, B., M.V. FINCO, M.D. NELSON, R.C. CZAPLEWSKI, E.H. HELMER, J.A. BLACKARD, G.R. HOLDEN, A.J. LISTER, D. SALAJANU, K. WEYERMANN, AND K. WINTERBERGER. 2008. Conterminous US and Alaska forest type mapping using Forest Inventory and Analysis data. *Photogramm. Eng. Remote Sens.* 74(11):1379–1388.

SCOTT, C.T., W.A. BECHTOLD, G.A. REAMS, W.D. SMITH, J.A. WESTFALL, M.H. HANSEN, AND G.G. MOISEN. 2005. Sample-based estimators used by the Forest Inventory and Analysis National Information Management System. P. 43–67 in *The Enhanced Forest Inventory and Analysis program—National sampling design and estimation procedures*, Bechtold, W.A., and P.L. Patterson (eds.). US For. Serv. Gen. Tech. Rep. SRS-80. 98 p.

TREUHAFT, R.N., B.E. LAW, AND G.P. ASNER. 2004. Forest attributes from radar interferometric structure and its fusion with optical remote sensing. *Bioscience* 54(6):561–571.

TURNER, D.P., W.B. COHEN, R.E. KENNEDY, K.S. FASSNACHT, AND J.M. BRIGGS. 1999. Relationships between leaf area index and Landsat TM spectral vegetation indices across three temperate zone sites. *Remote Sens. Environ.* 70(1):52–68.

US FOREST SERVICE. 2005. *Forest Inventory and Analysis Database documentation*. Available online at ncrs2.fs.fed.us/4801/fiadb/fiadb_documentation/FIADB_DOCUMENTATION.htm; last accessed Oct. 26, 2008.

US FOREST SERVICE. 2006. *The Forest Inventory and Analysis database: Database description and users guide version 2.1*. P. 211. Available online at fia.fs.fed.us/; last accessed Jan. 26, 2007.

US FOREST SERVICE. 2007. *FSGeodata clearinghouse*. Available online at svinetfc4.fs.fed.us; last accessed Oct. 26, 2008.

ZWALLY, H.J., B. SCHUTZ, W. ABDALATI, J. ABSHIRE, C. BENTLEY, A. BRENNER, J. BUFTON, J. DEZIO, D. HANCOCK, D. HARDING, T. HERRING, B. MINSTER, K. QUINN, S. PALM, J. SPINHIRNE, AND R. THOMAS. 2002. ICESat's laser measurements of polar ice, atmosphere, ocean, and land. *J. Geodyn.* 34(3–4):405–445.